Multireference Perturbation Theory Assessment of Electronic structure, and Reactivity for Iron-Doped Gold Clusters

Ali K. Almansori* and Falah S. Abd-Suhail**

***Department of chemistry, College of sciences, University of Kufa, Najaf,**

****College of pharmacy, The Islamic University, Najaf.**

alialmansori.aa@gmail.com

Abstract:

Doping a gold cluster with a transition metal atom allows the structural diversity of gold clusters to be combined with the distinctive features of high-spin systems. SMMs (single molecule magnets) are a special type of open-shell system with unique features. [1], by the complete active space self-consistent field methods We provided a map for HOMO-LUMO energy gaps to insight throw different complete active space CAS (e, o) compositions and different number of gold atoms structuring the studied clusters, along with binding energies correlation relationship with the studied cluster size.

Key words: CASSCF, Binding energy, HOMO-LUMO gap**.**

Introduction:

Gold clusters have attracted researchers' interest in cluster science for decades due to their applications in catalysis, electronic devices, biolabeling, and other domains. Because of their remarkable potential as a candidates in high-density data storage, the molecular origin of magnetism has accelerated the pace of research interest.[2] quantum computing [3] ,molecular spintronics[4], and fast magnetic switches [5][6] [7], Nanoalloys, which are made up of a mixture of two or more metals, provide technological and economic advantages over their pure metal alternatives.[8], The relevance of chemical composition and atomic arrangement is amplified when two metals are combined, which has a significant impact on physical and chemical

properties.[9], The size, structure, and composition of bimetallic clusters influence their electrical, optical, magnetic, and catalytic capabilities.[10], Noble metals like as Cu, Ag, and Au have a closed d shell and one valence electron in the s shell, and the minimal energy variation between the s and d shell results in strong hybridization effects, which help to compute the structure and electronic properties of these clusters.[11] Due to the obvious s–d hybridization of Au atoms in comparison to other coin-metals, Au clusters have a number of unique features.[12] [13]Their size-to-size structures are remarkable, as are their other interesting characteristics, such as chemical reactivity, great stability, and the ability to create them in a wide range of sizes and shapes.[14]The relativistic effects and metallophilic interactions of Au, in particular, result in gold clusters with unique geometric forms.[15][13] When compared to bulk gold, the characteristics of small to nano-sized gold clusters are very different [16].

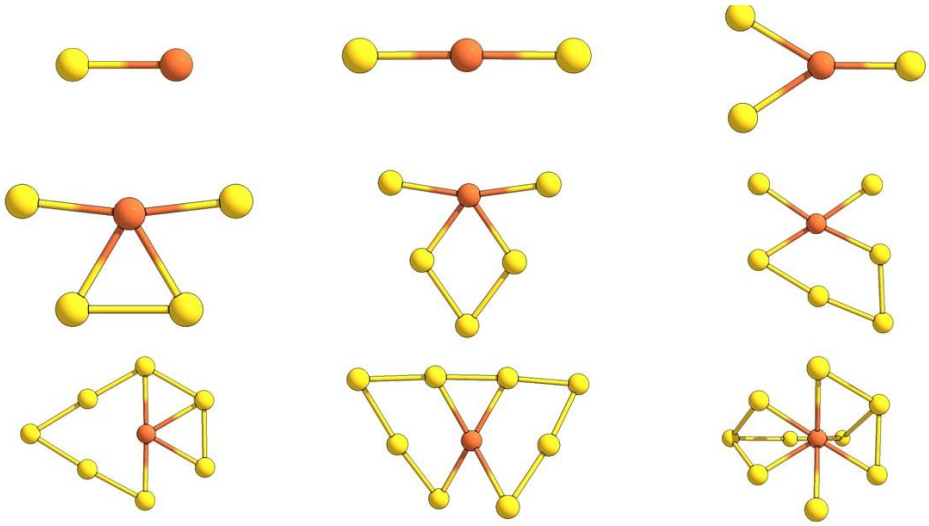

Interesting structural variants have been discovered, including two-dimensional flakes and three-dimensional compact, cage, and tube systems.[17][18], In addition, the geometries of small-sized Au clusters that exhibit planar structures within 13 atoms have been well located, while even more exotic structures, such as the Au_{20} pyramid and icosahedral Au_{32} cages, may have appeared at medium size.[19] Theoretical studies on nonmagnetic atom doping in magnetic clusters[20] and magnetic atom doping in nonmagnetic clusters[18] (atomicity < 12) reveal that the atom-cluster interaction mediated stability in the ground states and local electronic structures leads to an elevated magnetic moment.[6]

The influence of doping on the stability patterns of Au clusters, which are based on varying numbers of electrons that can be delocalized depending on the electronic configurations of the dopant atoms, has been the subject of several theoretical and experimental research. Zhao and Park used systematic DFT simulations to examine the structure evolutions of transition metal-doped gold clusters MAu12 (M = 3d–5d).[21].

HOMO-LUMO gap:

In particular, the HOMO-LUMO (Highest Occupied Molecular Orbital - Lowest Unoccupied Molecular Orbital) gap of these clusters plays a crucial role in determining their electronic behavior and optical properties.[22] The HOMO-LUMO gap represents the energy required to promote an electron from the highest occupied molecular orbital to the lowest unoccupied molecular orbital, and it determines the clusters' absorption and emission properties. Iron doping has been shown to affect the HOMO-LUMO gap of gold clusters, leading to changes in their electronic structure and optical properties. Understanding the factors that influence the HOMO-LUMO gap of iron-doped gold clusters is essential for designing and optimizing their performance in various applications, including catalysis, optoelectronics, and sensing[23]. In this paper, we investigate the HOMO-LUMO gap of iron-doped gold clusters using density functional theory (DFT) calculations and analyze the underlying electronic and structural factors that contribute to the observed changes in the HOMO-LUMO gap[24].

The binding energy of iron-doped gold clusters

The binding energy of iron-doped gold clusters refers to the energy required to remove an atom or molecule from the surface of the cluster, and it depends on various factors, such as the size, shape, composition, and electronic structure of the cluster. The binding energy is a critical parameter in catalysis, as it affects the adsorption and desorption of reactants and intermediates, thus influencing the overall catalytic activity. In this paper, we present a comprehensive study of the binding energy in iron-doped gold clusters using a combination of experimental and theoretical techniques[25]. We investigate the effects of iron doping on the binding energy of gold clusters and the role of cluster size and shape on the stability of these clusters. We also explore the electronic structure of the clusters and its contribution to the binding energy. Our results provide a better understanding of the factors that influence the binding energy in iron-doped gold clusters and their potential applications in catalysis and sensing[26].

Computational details:

The ORCA package[27], version 4.1.2, was used to run all the calculations in this study.[23] All optimized geometries were obtained using BP86 functional[28] with def2-TZVP basis sets for all atoms, in combination with the auxiliary basis sets of Weigend (def2/J). Subsequently, single point calculations were performed with various functionals to calculate exchange coupling constants using Noodleman formula. Convergence to the desired broken-symmetry states was confirmed by inspection of orbitals and spin populations. The broken symmetry approach is a computational method that involves modeling a molecule with broken spin symmetry[29]. In other words, the method assumes that the molecule has two or more distinct spin states, each with a different electronic configuration. This approach is particularly useful for molecules with unpaired electrons, such as radicals, which exhibit spin-dependent interactions. By breaking the spin symmetry, the approach allows for a more accurate description of the coupling constants in these systems. Moreover, complete active space method self-consistent field (CASSCF) method also was employed to test the validity of multi-reference in generating the coupling constants. To speed up the CASSCF calculations we have used RIJCOSX approximation. The N-electron valence perturbation theory (NEVPT2) in combination with the domain-based local pair natural orbital (DLPNO) were used to account for the dynamic correlation.[30]

Results and discussion:

HOMO-LUMO gap related reactivities:

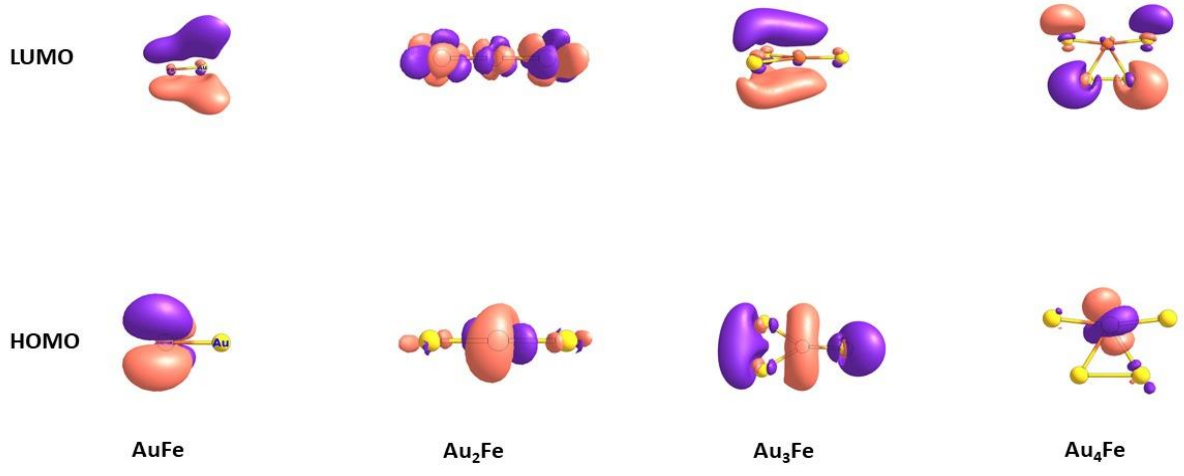

Figure 0.1: HOMO-LUMO orbitals for Co2L2Br2X complexes, L: tetraaza m-xylyl- ligand, X: H, O, OH, S bridging ligands.

for even electron count systems like (Au2Fe), (Au4Fe), (Au6Fe), and (Au8Fe) the composition of CAS (6,5) -meaning of 6 electrons in five orbitals- achieved best reasonable results, While the representative system AuFe magnetic properties was best investigated by CAS (7,11), the larger odd electron count systems (Au3Fe) (Au5Fe), and (Au7Fe) there best results calculated by CAS (9,8), our largest system (Au9Fe) was best treated with eleven electron in ten orbitals CAS (11,10).

Table 1: HOMO-LUMO energy gap for eight di cobaltous systems in eV

System	Gap (eV)	Occ	CAS
AuFe	36.63	0.01	7,11
Au2Fe	-93.03	1.2	9,8
Au3Fe	0.84	0.05	10,11
Au4Fe	-7.5	1.2	9,8
Au5Fe	0.02	0.12	9,8
Au6Fe	-49.33	1.2	6,5
Au7Fe	-0.6	0.26	6,5
Au8Fe	-6.91	1.2	6,5
Au9Fe	5.57	0.1	6,5

As the selected CAS compositions differs from a system to another, the electron density localization also differs between the selected active orbitals from 0.01- to 1.2 and hens the energy gap between HOMO-LUMO takes the range between (-93.03 To 36.63 eV), the previous table

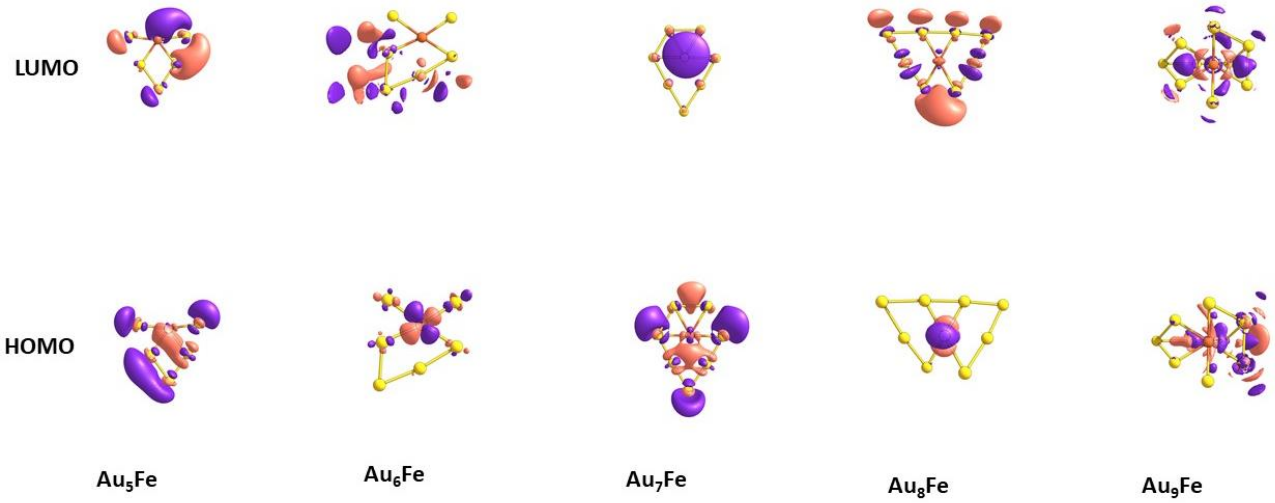

Figure 0.2: HOMO-LUMO orbitals for Co2L2Br2X complexes, L: tetraaza m-xylyl- ligand, X: SH, Cl, Br, I bridging ligands.

Iron doped gold clusters Binding energies (BE)

The variation of BEs as a function of cluster size is presented in Figure 0.3. This parameter can also be considered as the energy gained in assembling a definite cluster from isolated Au atoms and can be used to measure the thermodynamic stability of a cluster. The BEs for gold clusters up to Au_9 have been collected by means of DFT calculations,18,53

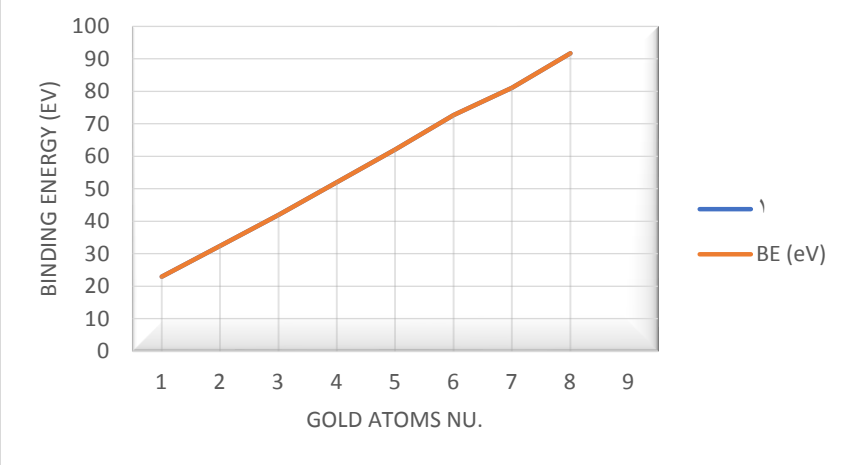

Figure 0.3: Binding energies per atom for neutral Au_n (n = 1−9) clusters as a function of cluster size. Results are obtained at the BP86/TZV(P) level.

As shown in Figure 0.3, the BEs of the Au_n clusters tend to increase when going from Au_1 to Au_8, exhibit a gradual growth and reach the maximal value of 91.7 eV/atom for Au_8Fe.

Conclusion

A map was generated for HOMO-LUMO energy gaps to get deeper insight by different complete active space CAS (e, o) set-ups, and different number of gold atoms structuring the studied clusters. While the correlation relationship between total binding energies and number of gold atoms in the studied cluster shown direct proportionality. We recommend for further investigation using unified CAS set-up for all systems to compare electron density distribution between the highest occupied molecular orbitals between all systems.

References:

[1] R. Sessoli, D. Gatteschi, A. Caneschi, and M. A. Novak, "Magnetic bistability in a metal-ion cluster," *Nature*, vol. 365, no. 6442, pp. 141–143, 1993.

[2] F. D. Natterer *et al.*, "Reading and writing single-atom magnets," *Nature*, vol. 543, no. 7644, pp. 226–228, 2017.

[3] M. N. Leuenberger and D. Loss, "Quantum computing in molecular magnets," *Nature*, vol. 410, no. 6830, pp. 789–793, 2001.

[4] F. Donati *et al.*, "Magnetic remanence in single atoms," *Science (1979)*, vol. 352, no. 6283, pp. 318–321, 2016.

[5] J. O. Johansson, J.-W. Kim, E. Allwright, D. M. Rogers, N. Robertson, and J.-Y. Bigot, "Directly probing spin dynamics in a molecular magnet with femtosecond time-resolution," *Chem Sci*, vol. 7, no. 12, pp. 7061–7067, 2016.

[6] D. K. Swain *et al.*, "Single Mn Atom Doping in Chiral Sensitive Assembled Gold Clusters to Molecular Magnet," *ACS Nano*, vol. 15, no. 4, pp. 6289–6295, Apr. 2021, doi: 10.1021/acsnano.0c10260.

[7] A. E. Green *et al.*, "Infrared Study of OCS Binding and Size-Selective Reactivity with Gold Clusters, Au n+ (n= 1–10)," *J Phys Chem A*, vol. 124, no. 26, pp. 5389–5401, 2020.

[8] G. Guzmán-Ramírez, J. Robles, and F. Aguilera-Granja, "Structure and electronic behavior of 26-atom Cu-Ag and Cu-Au nanoalloys," *The European Physical Journal D*, vol. 70, no. 9, pp. 1–7, 2016.

[9] D. Bochicchio and R. Ferrando, "Size-dependent transition to high-symmetry chiral structures in AgCu, AgCo, AgNi, and AuNi nanoalloys," *Nano Lett*, vol. 10, no. 10, pp. 4211–4216, 2010.

[10] R. Ferrando, J. Jellinek, and R. L. Johnston, "Nanoalloys: from theory to applications of alloy clusters and nanoparticles," *Chem Rev*, vol. 108, no. 3, pp. 845–910, 2008.

[11] C.-G. Li, Z.-G. Shen, Y.-F. Hu, Y.-N. Tang, W.-G. Chen, and B.-Z. Ren, "Insights into the structures and electronic properties of Cun+ 1 μ and CunS μ (n= 1–12; μ= 0,±1) clusters," *Sci Rep*, vol. 7, no. 1, pp. 1–11, 2017.

[12] S. Pande *et al.*, "Structural Evolution of Core–Shell Gold Nanoclusters: Au n–(n= 42–50)," *ACS Nano*, vol. 10, no. 11, pp. 10013–10022, 2016.

[13] Q. Liu, P. Fan, Y. Hu, F. Wang, and L. Cheng, "Superatomic and adsorption properties of Ni atom doped Au clusters," *Physical Chemistry Chemical Physics*, vol. 23, no. 18, pp. 10946–10952, May 2021, doi: 10.1039/d1cp00589h.

[14] P. V. Nhat, N. T. Si, and M. T. Nguyen, "Structural evolution and stability trend of small-sized gold clusters Au n (n= 20–30)," *J Phys Chem A*, vol. 124, no. 7, pp. 1289–1299, 2020.

[15] H. Schmidbaur and A. Schier, "Aurophilic interactions as a subject of current research: an up-date," *Chem Soc Rev*, vol. 41, no. 1, pp. 370–412, 2012.

[16] M.-C. Daniel and D. Astruc, "Gold nanoparticles: assembly, supramolecular chemistry, quantum-size-related properties, and applications toward biology, catalysis, and nanotechnology," *Chem Rev*, vol. 104, no. 1, pp. 293–346, 2004.

[17] D. M. P. Mingos, "Historical Introduction to Gold Colloids, Clusters and Nanoparticles," in *Gold Clusters, Colloids and Nanoparticles I*, Springer, 2014, pp. 1–47.

[18] C. Ehlert and I. P. Hamilton, "Iron doped gold cluster nanomagnets:: Ab initio determination of barriers for demagnetization," *Nanoscale Adv*, vol. 1, no. 4, pp. 1553–1559, 2019, doi: 10.1039/c8na00359a.

[19] M. P. Johansson, J. Vaara, and D. Sundholm, "On the aromaticity of small boron and gold clusters," *Angew. Chem*, vol. 116, p. 2732, 2004.

[20] M. Kabir, D. G. Kanhere, and A. Mookerjee, "Emergence of noncollinear magnetic ordering in small magnetic clusters: Mn n and As@ Mn n," *Phys Rev B*, vol. 75, no. 21, p. 214433, 2007.

[21] Q. Du *et al.*, "Structure Evolution of Transition Metal-doped Gold Clusters M@ Au12 (M= 3d–5d): Across the Periodic Table," *The Journal of Physical Chemistry C*, vol. 124, no. 13, pp. 7449–7457, 2020.

[22] S. F. Sousa, P. A. Fernandes, and M. J. Ramos, "General performance of density functionals," *Journal of Physical Chemistry A*, vol. 111, no. 42, pp. 10439–10452, Oct. 2007, doi: 10.1021/jp0734474.

[23] L. Mathivathanan *et al.*, "A trigonal prismatic Cu6-pyrazolato complex containing a μ6-F ligand," *Dalton Transactions*, vol. 44, no. 47, pp. 20685–20691, 2015, doi: 10.1039/c5dt03892h.

[24] E. V. Govor *et al.*, " A Redox-Induced Spin-State Cascade in a Mixed-Valent Fe 3 (μ 3 -O) Triangle ," *Angewandte Chemie*, vol. 129, no. 2, pp. 597–601, Jan. 2017, doi: 10.1002/ange.201610534.

[25] C. Adamo and D. Jacquemin, "The calculations of excited-state properties with Time-Dependent Density Functional Theory," *Chem Soc Rev*, vol. 42, no. 3, pp. 845–856, 2013.

[26] C. Ehlert and I. P. Hamilton, "Iron doped gold cluster nanomagnets:: Ab initio determination of barriers for demagnetization," *Nanoscale Adv*, vol. 1, no. 4, pp. 1553–1559, 2019, doi: 10.1039/c8na00359a.

[27] F. Neese, "Orca," *An ab initio, density functional and semiempirical program package version*, vol. 2, p. 19, 2009.

[28] H. Hirao, "Which DFT functional performs well in the calculation of methylcobalamin? Comparison of the B3LYP and BP86 functionals and evaluation of the impact of empirical dispersion correction," *Journal of Physical Chemistry A*, vol. 115, no. 33, pp. 9308–9313, Aug. 2011, doi: 10.1021/jp2052807.

[29] A. N. Georgopoulou *et al.*, "Site preferences in hetero-metallic [Fe9-: XNix] clusters: A combined crystallographic, spectroscopic and theoretical analysis," *Dalton Transactions*, vol. 46, no. 38, pp. 12835–12844, 2017, doi: 10.1039/c7dt02930f.

[30] Y. Jung, A. Sodt, P. M. W. Gill, and M. Head-Gordon, "Auxiliary basis expansions for large-scale electronic structure calculations," *Proceedings of the National Academy of Sciences*, vol. 102, no. 19, pp. 6692–6697, 2005.